The Photographic Infrared Absorption Spectrum of Gaseous Ammonia

SIU-HUNG CHAO,* *Ryerson Physical Laboratory, University of Chicago*

(Received March 2, 1936)

The photographic infrared absorption bands of ammonia at about 10,000A, 7920A, and 6470A have been measured with greater dispersion and resolving power than hitherto. Several series have been established in the first two bands by combination principle methods, but most of the band lines have not been classified. The complexity of structure occurs probably because each observed band is a composite of several parallel-type and perpendicular-type bands; the observed series, or most of them, probably constitute parallel bands. In the pure gas, the band lines are very sensitive to pressure, and do not become at all sharp until the latter is far below one atmosphere (cf. Fig. 1). In mixtures of ammonia and air, however, the air pressure produces very little broadening. The application of the combination principle to parallel, perpendicular, and Raman bands is discussed, taking into account the effects of unresolved but not negligible fine structure in the lines due to near-coincidence of lines of differing K values. Analysis of earlier data yields a rough value for a certain small rotational coupling coefficient and for the centrifugal deformation rotational coefficient, in the normal state of ammonia.

I. INTRODUCTION

THE absorption spectrum of the ammonia molecule, which belongs to the class of symmetrical top molecules, has been investigated in the infrared, visible and ultraviolet regions. The five bands in the photographic infrared and visible regions have been studied by the following investigators. Lueg and Hedfeld[1] reported having resolved 375 lines in the 10,230A band and 217 lines in the 8800A band, Badger and Mecke[2] reported 54 lines in the 7920A band and Badger[3] 57 lines in the 6470A band. The 5490A band has not been resolved. Because of the complexity of the structure, only partial analyses of these bands have been made. The present work[4] was undertaken in the hope of increasing the resolution in these bands, by using high dispersion and the special Eastman spectroscopic plates, so as to get accurately the rotational energy levels of the normal state of ammonia by a rigorous analysis according to the combination principle method, and to identify the upper vibrational levels of these bands.

In the present work, a higher resolution of these bands than previously has been attained. As an aid to the analysis, the constants of the rotational energy levels of the normal state of ammonia, found from the pure rotation band and from the Raman spectrum, were used. However, an analysis according to the combination principle method did not succeed very well. The difficulties and resulting conclusions will be stated in Section III.

II. REVIEW OF THEORETICAL CONSIDERATIONS[5]

The symmetry of ammonia is such that in equilibrium the molecule is a regular pyramid with three hydrogen atoms at the corners of an equilateral triangle. Dennison[6] showed that there should be four fundamental vibration frequencies, two belonging to nondegenerate symmetrical modes of vibration ("parallel-type" frequencies), and two degenerate frequencies, each corresponding to an unsymmetrical pair of modes of vibration ("perpendicular-type" frequencies).

The vibration bands may be divided into two types. In the "parallel" type, the electric moment oscillates parallel to the axis of symmetry. In the "perpendicular" type, it oscillates perpendicular to the axis. In ammonia, there should be two fundamental bands of the parallel type, say ν_1 and ν_3, and two fundamental bands of the perpendicular type, say ν_2 and ν_4, corresponding to the four fundamental frequencies.

The ammonia molecule in its equilibrium configuration belongs to the symmetry group C_{3v}. By group theory,[7] there exist three irreducible representations of this group, which have been called A_1, A_2 and E. Every vibrational wave

* Now at St. John's University, Shanghai, China.

[1] P. Lueg and K. Hedfeld, Zeits. f. Physik **75**, 599 (1932).

[2] R. M. Badger and R. Mecke, Zeits. f. physik. Chem. **B5**, 333 (1929).

[3] R. M. Badger, Phys. Rev. **35**, 1038 (1930).

[4] Preliminary account, S. H. Chao, Phys. Rev. **48**, 569*L* (1935).

[5] Cf. e.g., E. Teller, *IIand- und Jahrbuch der chemischen Physik*, Vol. **9–2** (1934).

[6] D. M. Dennison, Rev. Mod. Phys. **3**, 280 (1931).

[7] E. Wigner, *Göttinger Nachr. Math.-Phys. Klasse* (1930), p. 133; R. S. Mulliken, Phys. Rev. **43**, 279 (1933).

function of ammonia (neglecting the tunnel effect) must belong to one of these three representations. Of the three types, A_1 and A_2 are nondegenerate, while E is doubly degenerate. Of the four fundamental frequencies, the two nondegenerate can be shown to belong to representation A_1 and the two degenerate to representation E. Tisza[8] showed that the n-quantum overtones of frequencies of the types A_1 and E give vibrational states as follows:

$$[A_1{}^n]=A_1;$$
$$[E^n]=\begin{cases}E & \text{when } n \text{ is } 1,\\ A_1+E & \text{when } n \text{ is } 2,\\ A_1+A_2+E & \text{when } n \text{ is } 3; \text{ etc.}\end{cases} \quad (1)$$

Parallel bands can be shown to occur for transitions $A_1\leftrightarrow A_1$, $A_2\leftrightarrow A_2$, or $E\leftrightarrow E$, perpendicular bands for $A_1\leftrightarrow E$, $A_2\leftrightarrow E$, or $E\leftrightarrow E$. Since the normal state of ammonia is of type A_1, the four fundamental bands involving the normal state are $\nu_3(\|)=(A_1\leftarrow A_1)$, $\nu_4(\perp)=(A_1\leftarrow E)$, $\nu_1(\|)=(A_1\leftarrow A_1)$ and $\nu_2(\perp)=(A_1\leftarrow E)$.

As a result of the tunnel effect, in which the nitrogen atom can penetrate the potential barrier in the hydrogen triangle according to the quantum mechanics, each vibrational level as above classified is really split into two, denoted by α and β (symmetrical and antisymmetrical with respect to a central plane). There are selection rules as follows: (1) for the parallel type of band, $\alpha\leftrightarrow\beta$; (2) for the perpendicular type, $\alpha\leftrightarrow\alpha$ and $\beta\leftrightarrow\beta$; (3) for the Raman spectrum, $\alpha\leftrightarrow\alpha$ and $\beta\leftrightarrow\beta$.

It is now fairly certain[9] that the four fundamental bands of ammonia are as follows: 10.5μ, $\nu_3(\|)$; 6.13μ, $\nu_4(\perp)$; 3.0μ (ν_1, $\|$, overlapped by ν_2, $\perp$). Calculations by J. B. Howard[10] indicate that ν_2, $\perp$ should be at about 3450 cm^{-1}. Since such a band would overlap ν_1, $\|$ at 3.0μ, we have an explanation of the observed structure of the 3.0μ band which, although its strongest lines can be explained as ν_1, $\|$, with center at 3335 cm^{-1}, contains also many other lines. Further, M. Migeotte[11] has found in ND_3 a band analogous to the 3.0μ band of NH_3. This consists of two overlapping bands, one of parallel and one of perpendicular type, with the latter of somewhat lower frequency than the former.

The rotational energy of the symmetrical top rotator is given by

$$E_r=\frac{h^2}{8\pi^2}\left[\frac{J(J+1)}{I_A}+\left(\frac{1}{I_C}-\frac{1}{I_A}\right)K^2\right]+\cdots, \quad (2)$$

where $Jh/2\pi$ is the total angular momentum of the molecule and $Kh/2\pi$ is its component along the figure axis, I_C and I_A being the moments of inertia along and perpendicular to the symmetry axis. By substituting $B=h/8\pi^2cI_A$ and $\beta=(I_A/I_C)-1$, and assuming that the molecule is also deformed on account of rotation, the rotational energy in wave numbers is

$$F(J,K)\equiv E_r/hc=BJ(J+1)+\beta BK^2+DJ^2(J+1)^2+\cdots, \quad (3)$$

where $K\leqq J$. When the vibrational state is of a degenerate type, there is an interaction between the angular momentum vector K and the angular momentum associated with the vibration, giving rise to a correction term $\pm 2\beta' BK$ which must be added to Eq. (3).[12]

The selection rules for transitions between rotational energy levels are (1) for the parallel type of band, $\Delta J=0, \pm 1$ and $\Delta K=0$; (2) for the perpendicular type, $\Delta J=0, \pm 1$ and $\Delta K=\pm 1$; and (3) for the Raman spectrum, $\Delta J=0, \pm 1, \pm 2$ and $\Delta K=0$.

Because of the nuclear spin of the hydrogen atoms, the quantum weights of those levels with quantum number K divisible by three (including 0) are doubled. Besides this, there is a weight factor $2J+1$ for $K=0$, $2(2J+1)$ for $K>0$.

III. Search for ΔF's and Difficulties in Analysis; Nature of Bands

In order to analyze the photographic vibration-rotation bands by the combination principle method, it is desirable to know the ΔF's of the normal state. Perhaps the most fundamental type of ΔF is the double difference between rotational energy levels of equal K, given by

[8] L. Tisza, Zeits. f. Physik **82**, 48 (1933).

[9] The writer is greatly indebted to Professor D. M. Dennison for correspondence (also to M. Migeotte for information on ND_3) relating to this point.

[10] J. B. Howard, J. Chem. Phys. **3**, 207 (1935); see this paper also for earlier literature.

[11] Private communication to Professor Mulliken.

[12] E. Teller and L. Tisza, Zeits. f. Physik **73**, 791 (1933); M. Johnson and D. M. Dennison, Phys. Rev. **48**, 868 (1935).

$$\Delta_2 F_K(J) \equiv F_K(J+1) - F_K(J-1). \quad (4)$$

For ammonia these quantities can be obtained approximately from the pure rotation band and the Raman spectrum. Another type of ΔF of some importance is the single difference for fixed K, given by

$$\Delta_1 F_K(J) \equiv F_K(J+1) - F_K(J). \quad (5)$$

Still other types of ΔF's can be given, e.g.,

$$\Delta_2 F_J(K) = F_J(K+1) - F_J(K-1), \quad (6)$$

with J fixed.

According to the combination principle,[13] in a given vibration-rotation band, if $\Delta K = 0$, the difference of the wave numbers of a P and an R line involving a common upper rotational (and vibrational) level is

$$\Delta_2 F_K''(J) = R_K(J-1) - P_K(J+1), \quad (7)$$

where $\Delta_2 F_K''(J)$ is a difference between two lower rotational energy levels. Assuming the lower rotational levels given by Eq. (3), Eq. (4) now yields

$$\Delta_2 F_K''(J) = 2(2J+1)[B'' + 2D''(J^2+J+1)]. \quad (8)$$

From a study of observed $\Delta_2 F_K''(J)$'s, B'' and D'' could be evaluated.

From two lines with a common lower level, one finds for the upper rotational levels

$$\Delta_2 F_K'(J) = R_K(J) - P_K(J). \quad (9)$$

In the type of band where $\Delta K = 0$ and $\Delta J = 0$, ± 1 (parallel type infrared bands), each line is composed of several, usually superposed, components due to lines with the same J' and J'' but different values of K. Since $K \leqq J$, the number of superposed lines depends upon the value of J. A similar superposition of components exists also for Raman bands ($\Delta K = 0$, $\Delta J = 0$, ± 1, ± 2).

In attempting to apply Eqs. (7)–(9) to parallel type infrared bands (which includes the "pure rotation" bands as a special case), the compositeness of the lines, just mentioned, causes difficulty. Thus the $\Delta_2 F$'s obtained by applying Eqs. (7)–(9) represent some sort of averages over several K values. These average ΔF's for parallel bands may be called ΔF_{Pa}'s, and are defined, e.g., by

$$\Delta_2 F_{Pa}''(J) = R_{Pa}(J-1) - P_{Pa}(J+1) = F_{Pa}(J+1) - F_{Pa}(J-1), \quad (10)$$

where the symbol R_{Pa} or P_{Pa} refers to the measured frequency of a composite line.

To be sure, the quantities $R_K(J)$, $P_K(J)$, $\Delta_2 F_K(J)$ would be independent of K, and all components of a P or R line would coincide exactly, if Eqs. (3) and (8) were exact, but in practice, as we shall find, this is not quite true. The frequency which is measured for a line, corresponding evidently to the maximum of intensity of the observed composite line, obviously depends somewhat on the distribution of intensity among the different unresolved components (different K values) which make up the observed line. It is clear that, in general, any observed $\Delta_2 F_{Pa}''(J)$ value obtained from Eq. (10) should lie somewhere between the $\Delta_2 F_K(J)$ values with $K = 0$ and with $K = J$. Wright and Randall[14] and Barnes[15] in measuring the pure rotation band of ammonia, have obtained data allowing the evaluation of $\Delta_2 F_{Pa}''(J)$'s.

A similar situation exists for Raman effect ΔF's. In the pure rotation Raman effect, the observed Raman shifts are precisely $\Delta_1 F(J)$'s for $\Delta J = \pm 1$, and $\Delta_2 F(J)$'s for $\Delta J = \pm 2$. We may define

$$(\Delta J = \pm 1): \ \Delta_1 F_{Rm}(J) = \nu_{Rm}(J)_{\Delta J=1} = F_{Rm}(J+1) - \mathrm{F}(J), \quad (11)$$

$$(\Delta J = \pm 2): \ \Delta_2 F_{Rm}(J) = \nu_{Rm}(J-1)_{\Delta J=2} = F_{Rm}(J+1) - F_{Rm}(J-1). \quad (12)$$

Here again each ΔF is an average over several K values. The measured ν_{Rm} depends somewhat on the intensity distribution over the different K values. This can be shown to be different for the cases $\Delta J = \pm 1$ and ± 2 in the Raman effect, while $R(J-1) - P(J+1)$ in parallel type infrared bands is still different. Hence, unless the $\Delta_1 F_K(J)$'s and $\Delta_2 F_K(J)$'s are independent of K, one should find slight discrepancies between $\Delta_2 F_{Rm}(J)$ and $\Delta_2 F_{Pa}(J)$, and between $\Delta_2 F_{Rm}(J)$ and $\Delta_1 F_{Rm}(J-1) + \Delta_1 F_{Rm}(J)$.

In the Raman spectrum of ammonia, Lewis and Houston[16] found accurately not only $\Delta_2 F_{Rm}(J)$'s

[13] Cf. e.g., W. Jevons, *Band Spectra of Diatomic Molecules* (The Physical Society, London, 1932), p. 47.

[14] N. Wright and H. M. Randall, Phys. Rev. **44**, 391 (1933).

[15] R. B. Barnes, Phys. Rev. **47**, 658 (1935).

[16] C. M. Lewis and W. V. Houston, Phys. Rev. **44**, 903 (1933).

but also $\Delta_1 F_{Rm}(J)$'s. For the changes $\Delta J=\pm 2$, assuming $\Delta_2 F_{Rm}(J)$ to be given by the equation

$$\Delta_2 F_{Rm}(J)=2(2J+1)[B_0+2D_0(J^2+J+1)], \quad (13)$$

they found $B_0=9.92$ and $D_0=-0.00052$. If Eqs. (3) and (8) were exactly valid, the coefficients B_0, D_0 thus obtained should coincide with B'', D'' of Eqs. (3) and (8) as applied to the normal state of the molecule. However, the Raman shifts with $\Delta J=\pm 1$ calculated from these constants deviate systematically from the observed Raman shifts. The discrepancy may be accounted for in the following way.

As already noted, each line observed in the Raman spectrum is really composed of several components of differing K value, the number of which depends upon the value of J. From the formulas for calculating the theoretical intensities of the lines,[16] one finds that for a given observed line with $\Delta J=\pm 1$ the intensity of the components should be highest for the higher values of K. When $\Delta J=\pm 2$, however, the intensity of the components is highest for the smaller values of K.

Now suppose a small correction in the form $\alpha K^2 J(J+1)$ is added to Eq. (3). A correction of this form is to be expected theoretically. Eq. (3) then becomes

$$F(J, K)=(B+\alpha K^2)J(J+1) +\beta B K^2+DJ^2(J+1)^2. \quad (14)$$

When K varies from 0 to J, there is now a slight difference in frequency between the different K components of an observed line, although in practice these differences have been too small to resolve. Since the corrections are small, each observed line will correspond to the maximum intensity of the resultant of the different components. In order to determine the position of maximum intensity for this resultant, the intensity-frequency curve of each component was assumed to have a simple triangular form, whose base was made approximately twice the half-intensity breadth of the line, in such a way that the curves would overlap each other. The position of maximum intensity was then obtained by summing the individual intensities due to the different components, and should correspond to the frequency of the measured line in the Raman spectrum. Then the double difference for $\Delta J=2$ is

$$\Delta_2 F_{Rm}(J) =2(2J+1)[B''+2D''(J^2+J+1)+\alpha''\overline{K_2^2}], \quad (15)$$

and the difference between consecutive levels for $\Delta J=1$ is

$$\Delta_1 F_{Rm}(J) =2(J+1)[B''+2D''(J+1)^2+\alpha''\overline{K_1^2}], \quad (16)$$

where the bars denote averages. Values of $\overline{K_1^2}$ and of $\overline{K_2^2}$ obtained according to the procedure outlined above are given in Table I.

TABLE I. *Values of* $\overline{K_1^2}$ *and* $\overline{K_2^2}$.

J	$\overline{K_1^2}(\Delta J=1)$	$\overline{K_2^2}(\Delta J=2)$	J	$\overline{K_1^2}(\Delta J=1)$	$\overline{K_2^2}(\Delta J=2)$
0	0	0	5	16.9	3.4
1	1.4	0.2	6	24.0	7.0
2	3.2	0.4	7	33.0	8.0
3	6.2	0.6	8	44.0	10.0
4	10.9	1.3	9	57.5	11.0

If these values of $\overline{K_1^2}$ and $\overline{K_2^2}$ are plotted against J^2, it is found that the $\overline{K^2}$'s are approximately proportional to J^2, although there are some irregularities in the plot on account of doubling of the quantum weights of those levels for which K is a multiple of three (including 0). If we put $\overline{K_1^2}=cJ^2$ for $\Delta J=1$ and $\overline{K_2^2}=dJ^2$ for $\Delta J=2$, where c and d are constants of proportionality, the values of the constants are found to be approximately $c=0.69$ and $d=0.14$. Then the equations for the Raman shifts become

$$\Delta_2 F_{Rm}(J)=2(2J+1) \times[B''+2D''(J^2+J+1)+0.14\alpha''J^2] \quad (17)$$

and

$$\Delta_1 F_{Rm}(J)=2(J+1) \times[B''+2D''(J+1)^2+0.69\alpha''J^2]. \quad (18)$$

The values of c and d being known, α'' may be calculated from the difference between the *observed* $\Delta_1 F_{Rm}(J)$ Raman shifts, supposed to correspond to Eq. (18), and certain pseudo values of $\Delta_1 F_{Rm}(J)$ based on the observed $\Delta_2 F_{Rm}(J)$'s and calculated as if they were related to the latter as true $\Delta_1 F_K(J)$'s would be related to true $\Delta_2 F_K(J)$'s (cf. Eqs. (4), (5)). This difference is $2(c-d)\alpha''J^2(J+1)$. The best fit of the observed differences with this formula is obtained for $\alpha''=0.00154$. The probable error in this figure is, of course, relatively large. It should be men-

tioned especially that the observed differences do not fit the predicted form $CJ^2(J+1)$ very well.

By comparing Eq. (17) with the observed values of $\Delta_2F_{Rm}(J)$ from the Raman spectrum, taking $B''=9.92$, since B'' is evidently practically the same as B_0, D'' is found to be -0.00061. Thus in Eqs. (14)–(18) we have, for the normal state of ammonia, $B''=9.92$, $\alpha''=0.00154$, $D''=-0.00061$. Using Eqs. (4) and (14), we get

$$\Delta_2F_K''(J)=2(2J+1)\times[9.92-0.00123(J^2+J+1)+0.00154K^2]. \quad (19)$$

For parallel-type bands in the infrared spectrum (cf. Eq. (10)) the Eqs. (17) and (19) are replaced by

$$\Delta_2F_{Pa}''(J)=2(2J+1)\times[9.92-0.00123(J^2+J+1)+0.00154bJ^2], \quad (20)$$

where bJ^2 has been put in place of $\overline{K^2}$, b being similar to d of $\Delta_2F_{Rm}(J)$. On comparing the values calculated from Eq. (20) after omitting the last term in the bracket with those obtained from observed values of Barnes[15] in the pure rotation band of ammonia, the differences should be equal to $0.00308bJ^2(2J+1)$. Using Barnes' data, the value of b is found to be 0.45 and Eq. (20) becomes of the form

$$\Delta_2F_{Pa}''(J)=19.838+39.674J-0.00596J^2-0.00212J^3. \quad (21)$$

The value of b could also have been calculated from the intensity distribution of the K components in the lines of a parallel-type band, but this was not done here.

From Eqs. (19) and (21), double differences $\Delta_2F''(J)$ have been calculated for use in comparison with experimental data below. In the second and fourth columns, values of $\Delta_2F_K''(J)$ are given for $K=0$ and $K=J$; in the third column for a mean K^2 value corresponding to $\Delta_2F_{Pa}''(J)$.

For the perpendicular type band, the J double difference in wave numbers, with constant K, should be given by Eq. (19). If J is constant, the K double difference should be

$$\Delta_2F_J''(K)=\pm4\beta'B+4K[\beta B+0.00154J(J+1)]. \quad (22)$$

In analyzing the photographic bands of ammonia according to the combination principle

TABLE II.

J	$K=0$	$\overline{K^2}=bJ^2$	$K=J$
1	59.50 cm^{-1}	59.50 cm^{-1}	59.51 cm^{-}
2	99.12	99.15	99.18
3	138.66	138.74	138.84
4	178.10	178.30	178.54
5	217.40	217.78	218.25
6	256.55	257.20	258.00
7	295.50	296.52	297.77
8	334.23	335.81	337.58
9	372.72	374.85	377.46
10	410.90	413.81	417.38
11	448.80	452.67	457.39

method, it was attempted to select pairs of lines with wave number differences about equal to the known double differences $\Delta_2F_K''(J)$ or $\Delta_2F_{Pa}''(J)$ of the normal state and to arrange these into series, but this procedure gave only a few good series.

Then simple types of parallel and perpendicular bands predicted by assuming the rotational constants of the upper state levels not much different from those of the normal state were compared with the observed bands. Only the 6470A band seems to follow at all the general structure of the simple perpendicular type, but detailed consideration[4] did not confirm this structure. Then a parallel-type band with different B and β in the upper and lower states was tried[17] but the general appearance of the observed bands is far different from this type.

It seems very likely[9] that the difficulties in analyzing the bands may be explained as follows. As several authors have pointed out, the frequencies of the main photographic bands are approximately multiples of the frequency of the band at 3.0μ. For example, Adel[17] gives the equation $\nu_n=3389n-50n^2-2n^3$. But if the 3.0μ band is composed of *two* overlapping fundamental bands (cf. Section II), then the bands here under consideration may involve not only harmonics of both these fundamentals, but also a variety of combination bands. Furthermore, it is to be noted that harmonics of a perpendicular-type fundamental include in general a set of several parallel and perpendicular-type bands. Thus each of the "bands" here considered may be composed really of a number of superimposed bands, some of parallel and some of perpendicular type.

[17] Cf. A. Adel, Phys. Rev. **48**, 103 (1935).

For example (cf. (1) and selection rules), the 10,230A band should according to this explanation consist of three perpendicular and three parallel bands, the λ7920 band of four parallel and five perpendicular bands, and the λ6470 band of five parallel and seven perpendicular bands. Besides, an additional doubling may appear in each band due to the tunnel effect (α, β doubling). Only some such degree of complexity as this seems to offer a reasonable explanation of the richness and apparent irregularity of the lines in each band, and the difficulty in carrying out an analysis with the help of the combination principle.

IV. Experimental Work

The five absorption bands in the long wavelength photographic region of gaseous ammonia were photographed with a 21-foot grating (Paschen mounting), the dispersion being about 2.6A per mm in the first order. A glass absorption tube, 32 mm in diameter and 4.3 m long, with plane glass windows fused on the two ends, and a 500-watt projection lamp as a source of light, were used. Eastman spectroscopic plates of the following types were used throughout the work: types *C* and *F* for 6470A and 5490A, type *R* for 7920A, types *P* and *Q* for 8800A and type *Q* for 10,230A. The spectrograms were made first with the absorption path equal to the length of the tube. Then by reflecting light through the tube with a right-angled prism, the path was increased to double the length of the tube. The time of exposure varied greatly with the type of plate and the region of the spectrum, from one-hour exposures for the second-order spectrum of the 6470A band to 85-hour exposures for the first-order spectrum of the 10,230A band. The plates were hypersensitized in an ice-cooled bath of 4 percent ammonia solution and dried before an electric fan after being washed in alcohol. The tube was filled with ammonia gas from a small tank containing pure liquid ammonia, very kindly supplied by Professor W. C. Johnson of the Department of Chemistry. Experiments were also made at the temperature of solid CO_2 (-77°C), with which the absorption tube was packed during exposure, the ammonia pressure indicated being 14 mm. Only the strong lines of the 10,230A band then appeared on the plates, while those of the other bands were too weak to be photographed.

The ammonia absorption lines were compared with standard lines of the second and third order spectra from a 220-volt iron arc. The wave numbers in vacuum were calculated in the usual way, except that those of the lines beyond 10,000A were computed in the way indicated by Babcock[18] by extending the use of Kayser's *Tabelle der Schwingungszahlen*, in the neighborhood of 10,000A. From the best spectrograms the following numbers of lines were measured: 714 lines in 10,230A, 304 lines in 7920A and 162 lines in 6470A. Absorption lines (only a few in number) due to the water vapor band, 9420A, were identified and eliminated from the 10,230A band.

Complete tables of lines in wave numbers are given in the Appendix.

V. Pressure Broadening of the Ammonia Band Lines

When Badger[3] employed pressures of one to five atmospheres in photographing the ammonia 6470A band, he noticed that increasing the pressure of the gas broadened the absorption lines. All the ammonia lines in the photographic region show the same effect of broadening when the pressure is varied, and all appear to show the same degree of broadening at atmospheric pressure. In order to get the best resolution of the lines, it is important to know their width under various pressures.

The accompanying spectrograms of the 7920A band (cf. Fig. 1), of which only the central portions are reproduced, show the variation of the width of the absorption lines with pressure. The lines at 750 mm pressure are about 0.55A broad and at 95 mm they become fairly sharp. They become still sharper at still lower pressures. This is shown in the 10,230A band, where at a pressure of 14 mm when the temperature of the gas is -77°C, the line widths become extremely small. The widths of the lines depend much more upon pressure of the gas than upon path length. The different absorbing lengths under the same pressure show apparently the same degree of broadening.

[18] H. D. Babcock, Phys. Rev. **46**, 382 (1934).

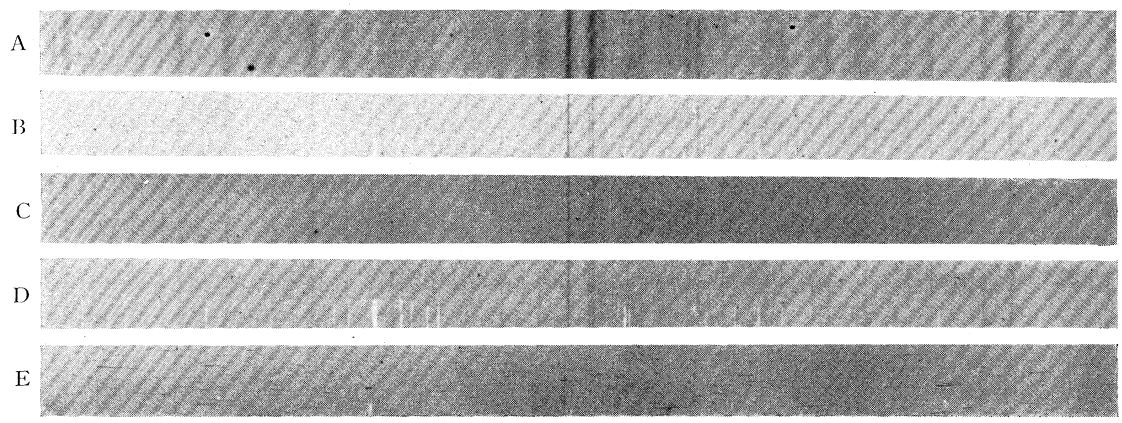

FIG. 1. 7920A band.

	A	*B*	*C*	*D*	*E*
Pressure (mm)	750	190	140	140+610 (air)	95
Absorption length (m)	4.3	8.6	8.6	8.6	4.3

The influence of a foreign gas (air) on the widths of the lines is shown in spectrogram (*D*), Fig. 1, for which air was admitted into the absorption tube containing ammonia at a pressure of 140 mm, making a total pressure of one atmosphere. The spectrogram of ammonia gas alone at 140 mm is also shown in (*C*), Fig. 1. In these two cases, the numbers of absorbing ammonia molecules are the same. Though there is a slight broadening effect of air on the absorption lines, this effect is very much smaller than that of the absorbing ammonia molecules on one another. The widths of the lines at 140 mm pressure plus 610 mm of air are shown nearly equal to those of the lines of ammonia alone at 190 mm.

In comparing the spectrogram of the ammonia lines at 750 mm pressure with that of the HCN absorption band 1.04μ at 630 mm and that of the HCl 1.20μ band, both obtained by Herzberg and Spinks,[19] the widths of the ammonia lines are smaller than those of the HCN lines but are about the same as those of the HCl lines. The widths of the HCN lines are about 1.4 times those of the ammonia lines at atmospheric pressure.

In the infrared spectrum of HCl, Lasareff[20] and Grasse[21] report that broadening of the absorption lines of the 3.46μ band caused by the presence of different gases is nearly the same as that caused by the absorbing gas (HCl) itself. They explained the phenomenon on the classical theory of Lorentz collision broadening. In ammonia, as well as in HCN, the pressure broadening of the lines cannot be attributed to this cause, but instead to intermolecular forces. It seems that the effect observed in ammonia may be explained in part by the intermolecular Stark effect due to the dipole moments of the molecules. Such an effect would be proportional to the dipole moment and to the number of molecules per cc.[22] The dipole moment of HCN is greater than those of NH_3 and HCl, the moments being 2.5–2.6, 1.44, and 1.03×10^{-18} e.s.u., respectively.[23]

An attempt has also been made to look for a dependence of the widths of the lines upon the quantum number J, but it appears that the effect, if any, must be comparatively small.

VI. Frequency Data and Analysis

10,230A and 8800A Bands

These two bands have been investigated by Lueg and Hedfeld,[1] but only a number of equal intervals in these bands were indicated by them. The 10,230A band appears in the present work to consist, as has not been noted previously, of

[19] G. Herzberg and J. W. T. Spinks, Proc. Roy. Soc. **A147**, 434 (1934); Zeits. f. Physik **89**, 477 (1934).
[20] W. Lasareff, Zeits. f. Physik **64**, 598 (1930).
[21] W. Grasse, Zeits. f. Physik **89**, 261 (1934).
[22] V. Weisskopf, Physik. Zeits. **34**, 1 (1933). See also H. Margenau, Phys. Rev. **48**, 755 (1935).
[23] Trans. Faraday Soc. **30**, following p. 904 (1934).

TABLE III. *Band:* $\nu_0 = 9760.38sb$.

Possible J	Possible P branch	Possible R branch	Possible $\Delta_2F''(J)$	Possible $\Delta_2F'(J)$
0		9779.85*s*		
		9780.39*s*		
1	9740.31*s*	9799.54*s*	59.58	59.23
	9741.22*sb*	9800.86*m*	59.13	59.64
2	9720.27*m*	9820.09*s*	99.16	99.82
	9721.26*s*	9820.92*s*	99.08	99.66
3	9700.38*m*	9840.13*s*	138.69	139.75
	9701.78*m*	9840.89*w*	138.59	139.11
4	9681.40*s*	9860.43*w*	178.80*	179.03
	9682.33*m*	9861.30*m*	178.67*	178.97
5	9661 33*sb*	9880.57*m*	217.67	219.24*
	9662.22*sb*	9881.95*w*	217.59	219.73*
6	9642.76*s*	9900.70*wb*	256.73	257.94
	9643.71*m*	9901.64*sb*	256.97	257.93*
7	9623.84*m*		295.90	
	9624.98*s*		295.70*	
8	9604.80*m*			
	9605.89*s*			

TABLE IV. *Band:* $\nu_0 = 10{,}099.74mb$.

Possible J	Possible P branch	Possible R branch	Possible $\Delta_2F''(J)$	Possible $\Delta_2F'(J)$
0		10,119.47*sb*		
1	10,079.84*mb*	10,139.31*sb*	59.71	59.47
2	10,059.76*mb*	10,159.17*w*	99.62*	99.41
3	10,039.69*s*	10,179.01*s*	139.17*	139.32*
4	10,020.00*s*	10,198.67*s*	178.92	178.67
5	10,000.09*s*	10,218.45*mb*	218.43*	218.36
6	9,980.24*w*			

TABLE V. *Band:* $\nu_0 = 10{,}104.86s$.

Possible J	Possible P branch	Possible R branch	Possible $\Delta_2F''(J)$	Possible $\Delta_2F'(J)$
0		10,125.31*s*		
1	10,084.77*m*	10,145.86*s*	60.49*	61.09
2	64.82*mb*	65.71*s*	102.17	100.89*
3	43.69*s*	85.98*sb*	142.49	142.29
4	23.22*m*	10,205.89*sb*	183.37	182.67*
5	02.61*sb*	26.37*m*	224.70	223.76*
6	9,981.19*s*	47.42*s*	266.52	266.23
7	59.85*s*		307.80	
8	39.62*s*			

two separate bands which can be distinguished by their intensity in absorption and which slightly overlap at 10,150A. The one of the longer wave-length is the stronger and its center is approximately at 10,230A. This stronger band has also been observed by Unger[24] using infrared technique. The center of the weaker band appears to be at 9900A.

On the high frequency side in the stronger band (10,230A), there are several groups of strong lines with intervals of about 10cm^{-1}, half the spacing characteristic of parallel-type infrared bands, suggesting a similarity to perpendicular type bands such as the 1.97μ band, studied by Stinchcomb and Barker, which also show 10 cm^{-1} spacings.

The strongest 200 lines, approximately, were taken from the 10,230A band and all pairs of lines with wave-number differences about equal to the double differences $\Delta_2F_{Pa}''(J)$ for $J=1$, 2, 3 and 4 were sorted out. For instance, taking the double difference for $J=3$ as about 138.7 cm^{-1} (cf. Table II), about ten pairs of lines giving $\Delta\nu$'s agreeing with this value to within ± 0.05 cm^{-1} were found. The most probable number[25] of accidental interval coincidences caused by random distribution of spectrum lines over 420 cm^{-1} (the approximate width of the band) is about 6, thus indicating that some but not nearly all of the $\Delta\nu$'s may represent real $\Delta_2F_{Pa}''(J)$'s. One series of close pairs of lines given in Table III gives $\Delta\nu$'s which agree very well with $\Delta_2F''(J)$'s given in Table II. The lines belonging to the series form arrangements like P and R branches of a parallel band (cf. Fig. 2, where the most likely J'' values are shown, preceded by a minus sign in the case of the P branch lines). The strong line in the center of the series corresponds to the Q branch (ν_0). No other series of lines giving $\Delta\nu$'s corresponding to Δ_2F'''s were found in the 10,230A band.

The structure of the 9900A band (cf. Fig. 3) is simpler than that of the 10,230A band. Two series of lines, given in Tables IV and V, were found in this band, one agreeing quite well with predicted $\Delta_2F''(J)$ values given in Table II, the other not agreeing with the predicted values though it forms a good series by itself.

The doublet series with $\nu_0 = 9760.38$ in the 10,230A band and the series with $\nu_0 = 10{,}099.74$ in the 9900A band presumably correspond to two of the three predicted parallel bands expected near 10,000A (cf. end of Section III). The doubling in the series with $\nu_0 = 9760.38$ is most likely the α, β (tunnel effect) doubling. The explanation of the band with $\nu_0 = 10{,}104.86$ is not obvious; it might involve an excited lower state, but seems too strong for this; besides, no temperature-sensitiveness was observed. Perhaps the arrangement in a series is spurious.

[24] H. J. Unger, Phys. Rev. **43**, 123 (1933).
[25] G. R. Harrison, Rev. Sci. Inst. **4**, 581 (1933).

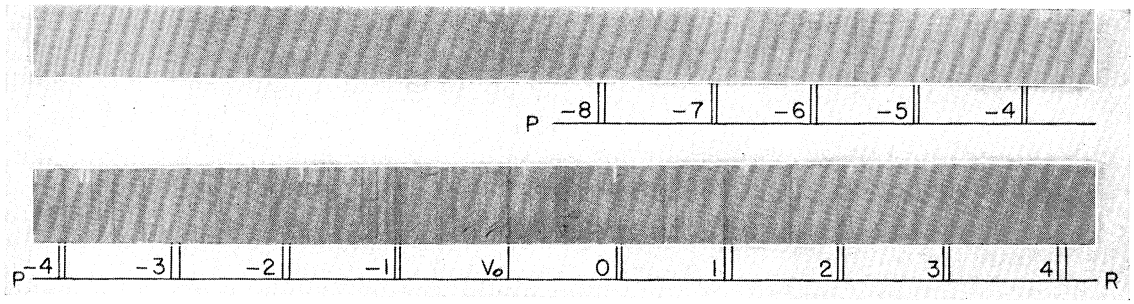

FIG. 2. 10,230A band. (v_0 should be ν_0.)

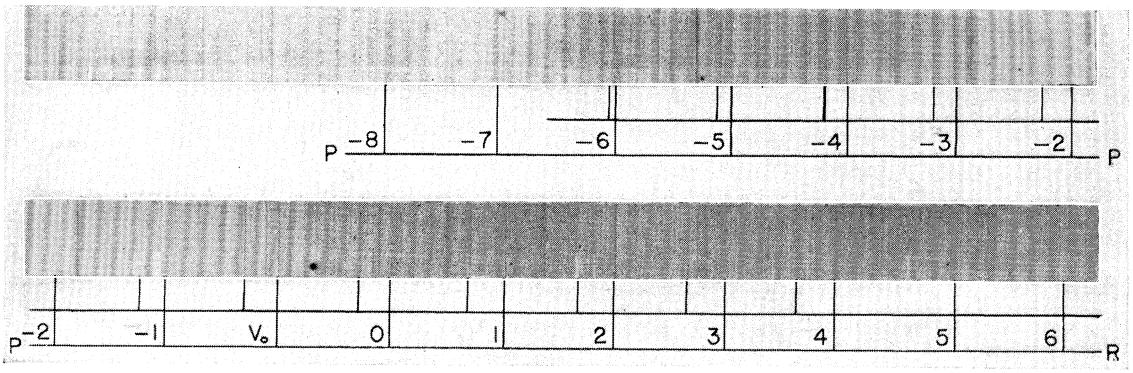

FIG. 3. 9900A band. (v_0 should be ν_0.)

The 8800A band was also photographed but because of the rapid falling off of sensitiveness of the plate in this region, it was not used for measurement.

In the preceding tables, the small letters following the wave number of each line denote its intensity, *viz.*, *ss*=very strong, *s*=strong, *m*=medium, *w*=weak and *b*=broad. The lines in series are arranged, and J values assigned, so as to give double differences as close as possible to the $\Delta_2 F_{Pa}''(J)$ values from Eq. (21), but the J numbering might still be shifted in some cases. The broad lines are usually due to blending of two or more lines and therefore their measurements are less reliable. When differences of observed $\Delta_2 F$'s from calculated values can be explained as due to blending with other lines, or to inaccuracy of measurement due to weakness of a line, they are marked with an asterisk.

7920A BAND

Badger and Mecke[2] found 54 lines in this band and arranged them into several series with a mean interval between adjacent lines equal to 19.88 cm^{-1}. They assumed the selection rule $\Delta K=\pm 1$, corresponding to the case of a perpendicular type band. Thus they took the spacing between the two strong lines in the center of the band with several lines in their neighborhood as the mean value of the coefficient of K^2 in Eq. (2), so that the moment of inertia, I_C, could apparently (but cf. Ref. 12) be evaluated.

In the present work an attempt was made to analyze the band rigorously by the combination principle method, but the structure does not fit the form either of a perpendicular type band or of a parallel type band. Two series, given in

TABLE VI. *Band:* $\nu_0=12{,}609.24s$.

POSSIBLE J	POSSIBLE P BRANCH	POSSIBLE R BRANCH	POSSIBLE $\Delta_2F''(J)$	POSSIBLE $\Delta_2F'(J)$
0		12,629.64*s*		
1	12,589.71*w*	49.33*sb*	59.73	59.62
2	69.91*s*	69.96*s*	99.07	100.05
3	50.26*m*	89.42*s*	138.73*	139.16
4	31.23*w*	12,708.95*s*	178.23	177.72
5	11.19*m*	29.12*m*	217.31*	217.93
6	12,491.64*w*	48.68*s*	257.32	257.04
7	71.80*w*	68.18*m*		296.38

TABLE VII. *Band:* $\nu_0 = 12{,}619.75s$.

POSSIBLE J	POSSIBLE P BRANCH	POSSIBLE R BRANCH	POSSIBLE $\Delta_2F''(J)$	POSSIBLE $\Delta_2F'(J)$
0		12,639.50*s*		
1	12,599.32*m*	58.65*s*	59.60	59.33
2	79.90*m*	79.19*sb*	99.20	99.29
3	59.45*sb*	98.37*m*	138.76	138.92
4	40.43*m*	12,718.86*s*	178.39	178.43
5	19.98*w*	37.62*s*	217.83	217.64
6	01.03*w*	56.29*s*	256.37	255.26
7	12,481.25*w*	75.71*m*		294.46

Tables VI and VII, were found, however. The $\Delta\nu$'s found in the two series agree with the double differences of the normal state as calculated from Eq. (21) (see Table II). The interval between the zero-lines of these two series is about 10 cm^{-1}.

It seems likely that the two series found in the 7920A band represent two of the four parallel bands expected in this region (cf. end of Section III).

6470A AND 5490A BANDS

Badger[3] has investigated these two bands and found 57 lines in the 6470A band, but he indicated only that the mean value of the spacing of the lines in series was 19.74 cm^{-1}. The structure of this band looks more like a perpendicular than a parallel type band. A group of strong lines which are nearly equally spaced in the center of the band suggests the Q branch of a perpendicular band, while there are also other groups of lines resembling P and R branches. However, on detailed consideration[4] it was not found possible to reconcile the structure with that expected for either a perpendicular or a parallel band. This is not surprising in view of the considerations given at the end of Section III.

The writer wishes to express his appreciation to Professor R. S. Mulliken for the proposal of the problem and for constant inspiration and valuable advice throughout the investigation, also to Professors D. M. Dennison and E. F. Barker for helpful correspondence. He also wishes to thank Professor G. S. Monk for valuable suggestions during the work and Professor W. C. Johnson for the pure liquid ammonia.

APPENDIX

10,230A and 9900A bands

Characteristics of the line are denoted as follows: *ss* = very strong, *s* = strong, *m* = medium, *w* = weak, and *b* = broad.

9503.74*w*	14.98*s*	84.58*w*	60.76*sb*	11.52*sb*	9868.58*w*	42.20*m*	12.56*sb*	82.90*mb*	56.10*w*
06.67*w*	16.09*w*	9685.63*s*	61.71*m*	13.03*s*	69.36*w*	42.66*m*	10013.75*s*	83.55*s*	57.02*m*
08.29*w*	17.49*w*	86.22*s*	62.87*w*	9814.03*mb*	70.18*s*	43.46*mb*	14.66*sb*	84.77*m*	10158.32*w*
10.57*w*	9618.88*w*	87.57*s*	63.39*s*	15.30*sb*	71.24*w*	9943.99*w*	16.29*s*	85.67*w*	59.17*w*
14.17*m*	20.56*w*	88.89*s*	9763.94*w*	16.97*s*	72.36*s*	44.66*m*	17.20*w*	10086.10*mb*	60.31*m*
9518.02*m*	21.34*m*	90.04*s*	64.51*s*	17.70*s*	9873.28*s*	46.06*s*	17.83*w*	86.76*m*	61.64*w*
22.94*m*	22.66*m*	9690.24*s*	65.46*m*	18.03*s*	73.95*s*	46.49*w*	10018.71*m*	87.86*w*	62.32*w*
28.60*m*	23.84*m*	90.84*w*	65.83*m*	9818.37*w*	76.01*s*	46.95*w*	19.45*m*	89.62*s*	10163.09*s*
33.80*s*	9624.98*s*	91.33*m*	66.37*s*	19.24*sb*	76.91*wb*	9947.47*w*	20.00*s*	90.18*s*	64.11*w*
34.26*w*	25.93*w*	91.80*sb*	9767.04*s*	20.09*s*	77.25*w*	48.94*w*	20.84*m*	10090.83*w*	64.57*w*
9534.66*m*	27.69*s*	93.20*m*	67.73*w*	20.42*w*	9877.83*w*	49.33*w*	21.72*w*	91.46*m*	65.71*s*
35.09*w*	28.94*m*	9694.11*m*	69.18*s*	20.92*s*	78.27*m*	49.95*w*	10022.55*m*	92.74*mb*	67.16*wb*
35.52*w*	29.38*m*	94.84*s*	69.91*m*	9821.53*s*	79.09*w*	50.50*m*	23.22*m*	94.46*mb*	10168.09*mb*
36.29*w*	9630.12*w*	95.43*s*	70.70*s*	22.41*sb*	79.76*m*	9950.92*s*	23.75*s*	95.07*s*	69.30*m*
37.06*m*	30.92*w*	96.40*m*	9771.35*s*	23.15*w*	80.57*m*	51.66*s*	24.23*m*	10096.57*mb*	69.84*w*
9538.40*m*	31.97*s*	97.35*m*	72.12*s*	23.83*s*	9881.95*w*	52.15*s*	25.48*mb*	97.32*mb*	70.40*w*
39.20*w*	32.54*s*	9698.32*m*	72.67*m*	27.54*m*	82.60*w*	53.12*m*	10025.91*w*	98.14*m*	71.34*w*
40.65*s*	33.10*w*	700.38*m*	73.38*s*	9828.19*w*	83.44*w*	53.94*w*	27.11*w*	98.74*s*	10172.17*w*
42.84*w*	9635.12*m*	01.78*m*	73.93*m*	28.86*m*	85.04*w*	9954.49*w*	27.53*w*	99.74*mb*	73.04*w*
44.93*w*	35.77*m*	02.48*m*	9774.70*m*	29.31*m*	85.76*w*	55.01*w*	28.61*w*	10100.74*s*	73.61*m*
9546.80*s*	36.40*mb*	03.22*m*	75.22*m*	29.91*sb*	9886.46*w*	55.83*m*	29.65*w*	02.56*s*	74.59*w*
47.45*m*	37.92*w*	9703.63*s*	75.87*w*	30.68*s*	87.77*w*	56.76*w*	10030.88*w*	03.27*s*	75.49*w*
52.28*s*	38.53*m*	04.59*s*	76.79*m*	9831.32*w*	88.64*w*	58.04*s*	31.73*m*	03.91*w*	10176.42*m*
52.71*w*	9639.57*s*	05.97*s*	77.56*mb*	31.91*m*	89.23*m*	9959.13*s*	32.65*s*	04.86*s*	79.01*s*
54.23*w*	40.14*s*	07.19*s*	9778.85*s*	32.39*m*	89.89*w*	59.85*s*	33.23*s*	10105.61*wb*	80.72*s*
9554.80*s*	41.17*m*	08.39*s*	79.08*s*	33.40*w*	9890.71*w*	61.08*s*	34.27*m*	06.90*s*	82.11*sb*
55.74*m*	41.92*s*	9709.15*s*	79.85*s*	33.82*m*	92.44*m*	61.81*s*	10035.14*m*	09.50*m*	82.79*w*
56.66*w*	42.76*s*	10.68*s*	80.39*s*	9834.40*w*	93.08*w*	63.74*s*	36.06*s*	10.18*m*	10184.46*w*
57.56*s*	0643.71*m*	12.31*m*	81.16*s*	34.63*w*	93.56*s*	9965.67*w*	36.87*m*	11.76*sb*	85.98*sb*
58.41*w*	44.60*mb*	13.92*s*	9781.89*w*	35.20*w*	94.42*w*	66.71*w*	37.44*sb*	10112.33*w*	89.02*w*
9562.48*s*	45.09*mb*	16.78*m*	82.61*m*	35.77*m*	9895.48*w*	68.72*w*	38.63*wb*	13.11*w*	89.84*w*
63.65*s*	45.94*mb*	9718.26*s*	83.09*s*	36.32*m*	96.84*mb*	69.94*w*	10039.69*s*	13.74*s*	90.77*w*
64.68*w*	46.61*mb*	19.23*s*	83.56*m*	9837.22*w*	97.73*s*	71.01*w*	40.55*m*	14.76*m*	10192.03*w*
65.33*m*	9649.87*s*	20.27*m*	84.19*w*	37.74*s*	98.57*w*	9972.33*sb*	41.21*wb*	16.93*s*	93.51*mb*
67.86*s*	50.98*s*	21.26*s*	9784.79*w*	39.13*s*	99.86*wb*	73.08*s*	42.56*wb*	10117.79*s*	93.95*w*
9569.54*s*	52.33*sb*	23.89*m*	85.29*w*	40.13*s*	9900.70*wb*	73.66*w*	43.69*s*	18.57*m*	95.92*sb*
70.96*s*	53.11*w*	9724.79*s*	85.44*w*	40.89*w*	01.64*sb*	74.10*w*	10044.85*w*	19.47*sb*	97.63*s*
73.23*m*	54.03*sb*	27.36*s*	86.38*w*	9841.58*w*	02.99*mb*	75.13*s*	45.88*s*	20.35*w*	10198.67*s*
74.74*s*	9654.34*sb*	28.40*s*	87.01*m*	42.18*w*	03.76*w*	9975.86*w*	46.58*s*	20.86*m*	202.35*s*
75.23*s*	55.80*w*	29.66*s*	9787.92*s*	42.86*s*	04.44*w*	76.51*m*	47.63*wb*	10121.87*m*	05.89*sb*
9576.05*w*	56.60*w*	30.22*s*	88.60*s*	43.45*s*	9905.36*w*	77.14*m*	48.59*wb*	22.98*s*	07.20*w*
76.39*m*	57.43*s*	9734.45*s*	89.96*s*	44.11*w*	06.46*s*	79.05*s*	10049.52*wb*	23.53*w*	09.14*m*
77.67*w*	59.07*m*	35.59*m*	90.75*s*	9844.78*m*	08.70*w*	79.60*w*	50.61*mb*	24.00*w*	10212.64*s*
78.54*m*	9660.00*w*	36.00*m*	91.17*m*	45.64*w*	09.44*w*	9980.24*w*	52.24*s*	24.55*m*	13.42*w*
79.50*w*	61.33*sb*	37.07*s*	9791.69*w*	46.41*m*	09.94*w*	81.19*s*	54.04*w*	10125.31*s*	14.63*s*

10,230A and 9900A bands—Continued

9580.60*s*	62.22*sb*	38.78*mb*	92.11*w*	47.43*s*	9910.38*m*	82.76*wb*	54.71*w*	26.18*s*	15.43*w*
82.43*s*	64.43*w*	9740.31*s*	93.24*s*	49.12*s*	11.23*mb*	83.73*w*	10055.29*w*	26.82*s*	17.19*wb*
83.34*s*	65.12*w*	40.72*sb*	93.64*m*	9849.40*w*	12.60*m*	84.26*w*	56.10*s*	27.70*w*	10218.45*mb*
86.29*s*	9665.92*s*	41.22*sb*	94.86*s*	50.11*s*	13.47*m*	9984.73*w*	57.05*w*	28.38*m*	19.84*sb*
87.66*s*	66.29*s*	42.15*w*	9795.38*w*	51.03*w*	14.50*s*	85.94*w*	57.29*w*	10129.27*m*	20.35*w*
9587.99*m*	67.15*m*	42.52*w*	95.86*m*	52.13*w*	9915.53*w*	86.63*s*	58.38*w*	30.70*mb*	21.39*w*
89.42*s*	68.52*w*	9743.32*m*	96.55*s*	52.47*w*	17.05*s*	87.96*w*	10058.83*w*	32.43*m*	22.63*mb*
91.12*w*	69.28*m*	43.83*m*	97.00*w*	9853.63*mb*	18.97*s*	89.26*s*	59.76*mb*	35.39*sb*	10225.46*wb*
91.64*s*	9670.11*s*	44.81*w*	97.30*w*	54.16*w*	20.48*w*	9990.32*w*	60.35*w*	38.72*sb*	26.37*m*
93.77*s*	71.58*w*	45.39*m*	9797.61*w*	55.28*m*	22.03*m*	91.64*s*	61.66*w*	10139.31*sb*	27.63*m*
9594.84*w*	72.14*w*	46.30*w*	98.11*w*	56.36*m*	9923.61*m*	92.72*m*	63.21*w*	41.24*w*	28.58*w*
95.40*w*	72.98*s*	9747.80*s*	98.92*w*	57.44*w*	25.41*s*	93.53*m*	10064.82*mb*	41.95*w*	29.98*w*
96.10*m*	73.58*s*	48.57*s*	99.54*s*	9857.93*s*	26.17*w*	94.67*m*	65.95*w*	42.65*w*	10230.53*s*
97.64*m*	9674.16*s*	49.50*m*	9800.12*m*	58.38*s*	26.83*w*	9995.51*m*	67.13*s*	43.17*w*	31.91*w*
601.27*w*	74.98*w*	50.10*w*	9800.86*m*	59.22*w*	29.62*s*	96.34*s*	67.98*m*	10143.96*s*	32.50*s*
9603.70*s*	75.76*s*	50.70*s*	01.39*w*	59.53*w*	9930.93*s*	98.19*w*	68.60*s*	44.52*s*	33.57*s*
04.80*m*	76.36*s*	9750.95*w*	01.99*w*	60.43*w*	32.15*w*	98.99*m*	10069.36*m*	45.86*s*	34.11*w*
05.33*w*	76.65*s*	52.04*m*	02.96*w*	9861.30*m*	33.06*w*	99.63*m*	70.01*m*	46.64*m*	10234.60*w*
05.89*s*	9678.39*s*	52.66*m*	03.45*w*	61.43*w*	34.77*m*	10000.09*s*	71.59*m*	47.35*m*	47.42*s*
06.98*m*	78.75*s*	53.46*s*	9804.19*m*	62.19*w*	36.61*sb*	00.61*s*	73.45*sb*	10147.71*s*	48.11*w*
9608.38*m*	79.64*s*	54.39*s*	05.19*m*	62.84*w*	9937.97*sb*	02.61*sb*	74.75*s*	48.48*w*	53.14*w*
08.95*s*	80.13*w*	9755.53*s*	06.59*s*	63.33*w*	38.47*w*	07.06*s*	10077.02*mb*	49.02*m*	
09.80*w*	80.78*s*	56.61*s*	07.72*s*	9863.74*s*	39.09*w*	07.62*s*	78.47*mb*	50.23*w*	
11.57*s*	9681.40*s*	58.19*mb*	08.50*w*	64.19*w*	39.62*s*	10008.89*s*	79.84*mb*	51.70*w*	
12.32*w*	82.33*m*	59.24*s*	9808.66*s*	65.04*w*	40.47*s*	09.52*sb*	80.95*s*	10152.59*sb*	
9613.13*w*	82.95*m*	59.80*s*	09.83*sb*	66.10*s*	9941.05*s*	10.35*s*	81.44*s*	54.12*w*	
13.52*m*	83.91*m*	9760.38*sb*	10.56*s*	67.06*mb*	41.51*w*	11.13*s*	10082.30*w*	55.23*m*	

7920A band

12454.35*w*	11.19*m*	49.61*w*	83.42*sb*	12.27*m*	12637.33*w*	65.07*w*	99.52*m*	25.91*w*	64.30*s*
64.55*w*	11.82*m*	50.26*m*	85.58*w*	12612.81*m*	37.98*w*	66.32*sb*	700.86*m*	26.43*s*	12765.55*m*
65.93*w*	12.99*m*	51.89*mb*	12587.24*w*	13.19*w*	38.99*s*	67.85*m*	01.66*m*	12727.76*s*	66.22*m*
67.20*w*	14.64*m*	12552.92*w*	88.42*w*	13.73*s*	39.50*s*	68.74*w*	12702.39*m*	29.12*m*	68.18*m*
68.24*w*	12515.88*m*	54.49*s*	88.81*sb*	14.54*m*	40.76*m*	12669.96*s*	03.22*w*	30.48*m*	68.90*m*
12469.77*mb*	17.11*s*	54.84*s*	89.71*w*	14.94*m*	12641.48*m*	70.84*m*	04.04*w*	31.13*s*	71.30*m*
71.80*w*	18.48*m*	56.28*sb*	91.25*w*	12616.06*m*	42.15*m*	71.14*m*	04.61*w*	31.48*s*	12772.78*m*
76.71*w*	19.98*w*	58.12*w*	12592.01*w*	17.23*sb*	43.61*s*	72.22*sb*	05.61*s*	12732.78*m*	75.71*m*
77.59*w*	21.71*sb*	12558.60*w*	92.80*m*	18.48*w*	44.03*m*	73.72*sb*	12706.98*w*	33.70*m*	77.80*m*
77.98*w*	12522.72*w*	59.45*sb*	94.23*m*	19.49*w*	45.21*s*	12675.46*w*	07.92*m*	35.68*m*	80.06*w*
12479.94*w*	24.16*m*	60.75*m*	94.64*m*	19.75*s*	12646.32*w*	76.29*w*	08.57*s*	36.09*s*	81.15*w*
81.25*w*	25.46*mb*	62.18*sb*	95.98*s*	12620.72*m*	47.23*w*	77.15*sb*	08.95*s*	37.62*s*	12782.25*m*
84.41*w*	26.87*mb*	62.96*w*	12596.44*s*	21.53*m*	48.36*w*	79.19*sb*	10.22*m*	12739.15*s*	84.45*m*
84.94*w*	28.12*w*	12564.44*w*	97.61*m*	22.50*w*	49.33*sb*	81.24*m*	12710.78*m*	39.84*s*	88.06*w*
85.66*w*	12529.46*w*	66.00*m*	98.81*m*	12624.36*ss*	50.08*m*	12682.07*m*	11.57*s*	40.88*s*	89.84*w*
12490.31*w*	30.29*m*	66.81*w*	99.32*m*	25.35*w*	12651.74*mb*	82.85*s*	12.18*m*	41.82*m*	94.43*w*
91.64*w*	31.23*w*	68.11*w*	600.08*w*	12626.38*w*	53.52*w*	83.76*w*	12.67*m*	44.16*m*	12797.47*w*
92.47*w*	33.53*w*	69.60*s*	12600.58*w*	12627.73*ss*	54.29*w*	84.87*m*	13.97*s*	12744.92*m*	800.62*w*
93.72*w*	36.17*mb*	12569.91*s*	01.24*w*	12628.30*ss*	55.30*s*	85.80*m*	12714.82*s*	45.49*m*	02.20*w*
94.88*w*	12537.49*w*	73.68*w*	01.54*m*	28.66*w*	55.86*s*	12686.89*w*	15.45*m*	46.02*s*	05.30*w*
12496.12*w*	38.62*mb*	74.78*m*	02.56*s*	29.07*m*	12656.52*s*	88.32*m*	16.66*m*	46.94*s*	06.19*w*
97.87*m*	39.83*w*	75.82*w*	03.08*s*	12629.64*s*	57.23*w*	89.42*s*	17.61*s*	47.87*s*	12807.64*w*
99.21*w*	40.43*m*	76.23*w*	12604.15*m*	30.16*s*	57.54*w*	91.50*s*	18.86*s*	12748.68*s*	09.46*w*
501.03*w*	41.39*w*	12576.89*w*	05.54*m*	31.33*s*	58.20*w*	93.20*m*	12719.31*s*	50.61*s*	09.63*w*
02.25*w*	12542.20*sb*	77.48*w*	06.04*m*	32.96*s*	58.65*s*	12694.01*m*	20.33*m*	52.46*s*	21.77*w*
12503.20*w*	43.96*s*	79.42*w*	07.38*w*	33.19*s*	12659.78*m*	95.57*s*	21.10*m*	54.46*s*	
04.94*w*	44.35*s*	79.90*m*	07.96*m*	12633.89*m*	61.28*w*	95.87*s*	22.83*s*	55.36*s*	
05.65*w*	44.68*s*	80.31*m*	12609.05*w*	34.48*m*	61.96*w*	96.43*w*	23.20*s*	12756.29*s*	
06.53*m*	46.31*m*	12581.56*w*	09.24*s*	35.31*w*	62.77*s*	97.06*s*	12723.93*w*	59.87*m*	
08.01*m*	12547.36*w*	82.12*w*	10.59*m*	36.10*s*	63.65*s*	12698.37*m*	24.32*w*	60 64*m*	
12509.82*mb*	48.36*sb*	82.74*m*	11.44*w*	36.58*m*	12663.83*w*	99.02*m*	25.29*m*	63.59*m*	

6470A band

15263.8*w*	29.7*m*	65.9*m*	97.2*m*	21.6*w*	15442.8*m*	72.3*m*	03.5*w*	29.7*s*	65.5*w*
68.6*w*	31.8*m*	15367.2*w*	98.2*w*	23.4*m*	44.5*s*	73.5*w*	15506.3*s*	30.8*w*	69.3*w*
72.3*m*	36.2*m*	68.2*m*	401.5*w*	15425.1*m*	46.8*s*	74.4*m*	08.2*s*	31.7*w*	15570.4*w*
89.4*w*	15339.3*m*	69.4*w*	02.8*m*	26.2*w*	47.8*w*	15477.8*m*	10.2*s*	32.6*w*	75.4*w*
94.6*w*	41.1*w*	70.4*w*	15404.4*s*	27.6*m*	48.8*w*	78.9*m*	12.5*s*	15533.4*w*	76.1*w*
15295.9*w*	42.4*w*	72.4*w*	05.5*w*	28.6*m*	15449.9*s*	82.4*s*	14.4*m*	34.8*s*	96.0*w*
300.2*m*	47.6*w*	15376.4*s*	08.2*s*	29.4*s*	50.8*m*	85.4*m*	15515.4*w*	35.9*m*	99.3*w*
02.2*w*	49.3*w*	78.7*w*	09.1*w*	15431.5*m*	52.5*s*	88.9*s*	16.5*s*	39.0*s*	15605.5*w*
04.2*w*	15351.3*w*	80.3*s*	10.0*w*	32.4*w*	53.7*w*	15489.9*s*	17.6*m*	41.1*m*	06.2*w*
07.5*w*	53.1*s*	83.3*s*	15411.1*w*	33.8*w*	55.5*m*	91.0*w*	18.9*s*	15543.9*w*	
15310.4*w*	54.3*s*	85.6*m*	12.2*w*	34.7*w*	15457.8*m*	92.0*w*	20.0*w*	45.7*w*	
16.4*w*	55.7*w*	15386.6*w*	13.9*m*	35.9*w*	58.7*w*	93.3*s*	15522.0*w*	48.4*m*	
17.2*w*	56.5*w*	87.6*s*	15.1*m*	15437.6*w*	59.9*m*	94.5*w*	22.7*w*	49.6*w*	
20.2*w*	15358.5*s*	90.6*s*	16.5*w*	38.1*m*	62.7*s*	15497.1*s*	23.9*w*	52.2*m*	
20.7*w*	61.9*m*	94.2*m*	15417.6*m*	39.4*w*	64.8*w*	99.6*s*	25.2*w*	15555.3*w*	
15324.3*w*	63.0*m*	95.0*w*	18.4*w*	40.2*m*	15466.0*m*	15501.5*m*	26.4*s*	57.8*w*	
26.4*w*	64.8*m*	15395.9*w*	20.0*s*	41.2*s*	66.9*m*	02.3*w*	15528.3*s*	59.3*w*	

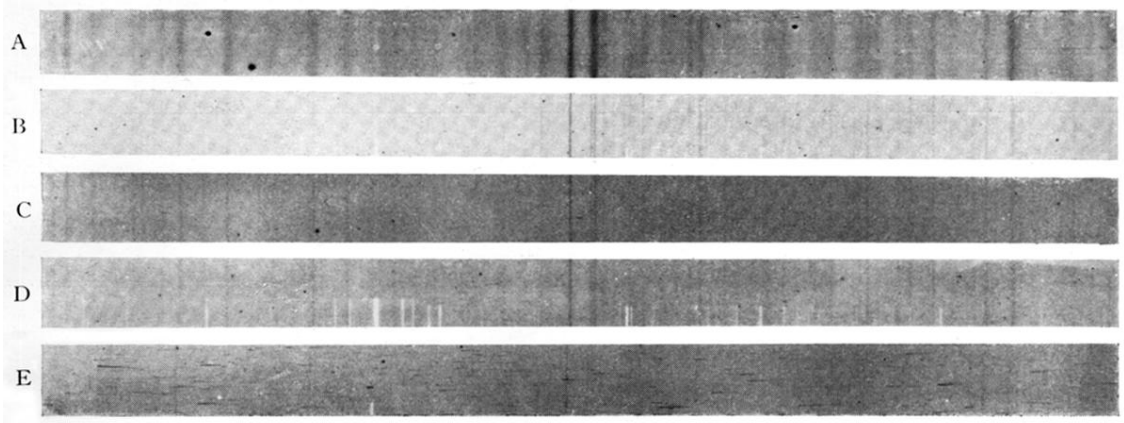

FIG. 1. 7920A band.

	A	*B*	*C*	*D*	*E*
Pressure (mm)	750	190	140	140+610 (air)	95
Absorption length (m)	4.3	8.6	8.6	8.6	4.3

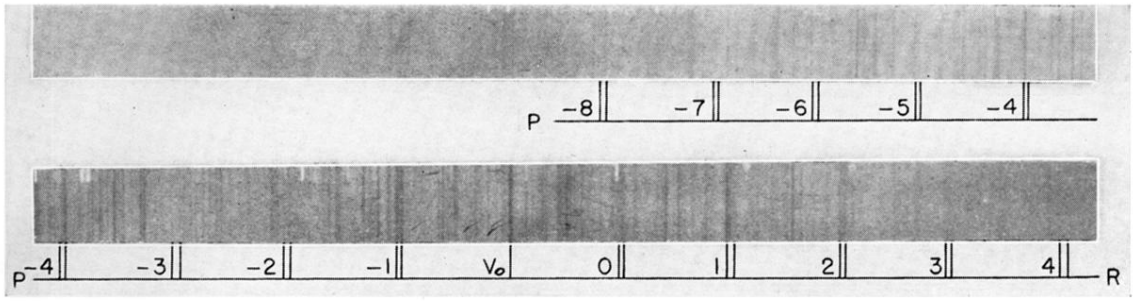

FIG. 2. 10,230A band. (v_0 should be ν_0.)

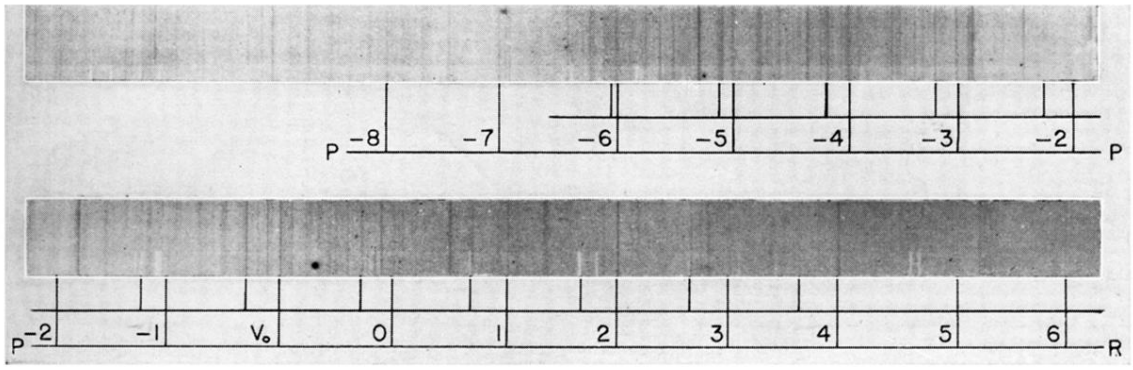

FIG. 3. 9900A band. (v_0 should be ν_0.)